THE JOURNAL OF COMPARATIVE NEUROLOGY 433:426–436 (2001)

Neuronal Plasticity and Formation of New Synaptic Contacts Follow Pyramidal Lesions and Neutralization of Nogo-A: A Light and Electron Microscopic Study in the Pontine Nuclei of Adult Rats

STEFAN BLÖCHLINGER, OLIVER WEINMANN, MARTIN E. SCHWAB, AND MICHAELA THALLMAIR*

Brain Research Institute, University of Zurich and Swiss Federal Institute of Technology-Zurich, CH-8057 Zurich, Switzerland

ABSTRACT

Regeneration and compensatory sprouting are limited after lesions in the mature mammalian central nervous system in contrast to the developing central nervous system (CNS). After neutralization of the growth inhibitor Nogo-A, however, massive sprouting and rearrangements of fiber connections occurred after unilateral pyramidal tract lesions in adult rats: Corticofugal fibers from the lesioned side crossed the midline of the brainstem and innervated the contralateral basilar pontine nuclei. To determine whether these newly sprouted fibers formed synaptic contacts, we analyzed the corticofugal fibers in the basilar pontine nuclei contralateral to the lesion by light and electron microscopy 2 weeks after pyramidotomy and treatment with the Nogo-A-inhibiting monoclonal antibody IN-1 (mAb IN-1). The mAb IN-1, but not a control antibody, led to structural changes in the basilar pons ipsilateral and contralateral to the lesion site. Fibers sprouted across the pontine midline and terminated topographically. They established asymmetric synaptic contacts with the characteristics of normal corticopontine terminals. These results show that adult CNS fibers are able to sprout and to form new synaptic contacts after a lesion when a growth-permissive microenvironment is provided. J. Comp. Neurol. 433:426–436, 2001.

Indexing terms: compensatory sprouting; neutralizing antibody; basilar pons; synapse; axotomy; ultrastructure

Regenerative and compensatory plastic fiber growth after lesions is restricted to short distances in the adult mammalian central nervous system (CNS). CNS tract lesions, therefore, lead to permanent functional impairment. This limited anatomical and functional repair in the mature CNS contrasts with the situation in the immature CNS, in which regeneration and compensatory sprouting of lesioned and unlesioned fibers can take place, and functional deficits are small (Kennard, 1936, 1938; Kalil and Reh, 1982; Kartje-Tillotson et al., 1986; Whishaw and Kolb, 1988; Barth and Stanfield, 1990; Kuang and Kalil, 1990).

The importance of myelin and the myelin-associated neurite growth inhibitor Nogo-A in preventing regenerative and compensatory fiber growth in the adult mammalian CNS has been well described (Caroni and Schwab, 1988a,b; Schwab et al., 1993; Kapfhammer, 1997; Chen et al., 2000). After corticospinal tract (CST) lesions, neutralization of Nogo-A by the monoclonal inhibitor-neutralizing antibody 1 (mAb IN-1) enhanced long-distance regeneration of adult corticospinal axons and recovery of locomotor functions (Schnell and Schwab, 1990, 1993; Bregman et

Grant sponsor: Swiss National Science Foundation; Grant numbers: 31-45549.95/2 and 4038-43918.95/2; Grant sponsor The Spinal Cord Consortium of the Christopher Reeve Paralysis Foundation; Grant sponsor: The International Research Institute for Paraplegia; Grant sponsor: The Velux Foundation; Grant sponsor: The Biotechnology Program of the European Union; Grant sponsor: Mr. Joachim Huber (private donation).

*Correspondence to: Dr. Michaela Thallmair, Laboratory of Genetics, The Salk Institute for Biological Studies, 10010 North Torrey Pines Road, La Jolla, CA 92037. E-mail: thallmair@salk.edu

Received 14 July 2000; Revised 14 November 2000; Accepted 12 February 2001

al., 1995). In addition, compensatory sprouting of lesioned axons and of corresponding unlesioned neurites after a unilateral pyramidotomy in adult rats treated with mAb IN-1 was observed in several studies (Thallmair et al., 1998; Z'Graggen et al., 1998; Raineteau et al., 1999). Nogo antibody-induced sprouting is thought to play an important role for the functional recovery seen in these animals (Thallmair et al., 1998; Z'Graggen et al., 1998). Anatomically, sprouting fibers from the lesioned pyramidal tract were seen to cross the midline and innervate the contralateral basilar pons and red nucleus in a topographically specific pattern (Thallmair et al., 1998; Z'Graggen et al., 1998). This finding is of special interest, because the newly formed projections innervate a region that was not denervated by the lesion and, thus, contained no vacant synaptic sites. Here, we show by electron microscopy that these sprouted, midline-crossing fibers established synapses with the typical characteristics of corticopontine synaptic terminals.

MATERIALS AND METHODS

Animals and surgery

Unilateral lesions of the CST at the level of the medulla oblongata (pyramidotomy) were performed in male Lewis rats at 8–10 weeks of age. The animals were divided into the following experimental groups: 1) tracing only (n = 3 rats), 2) lesion only (n = 2 rats), 3) lesion and anti-horseradish peroxidase (anti-HRP) antibody treatment (n = 3 rats), and 4) lesion and IN-1 antibody treatment (n = 6 rats). Rats were anesthetized by an intraperitoneal (i.p.) injection of Hypnorm (0.3 mg/kg body weight; Janssen, Buckinghamshire, England) and Dormicum (0.6 mg/kg body weight; Roche, Reinach, Switzerland). The medullary pyramids were exposed by a ventral approach through an opening of the occipital bone, as described earlier (Thallmair et al., 1998). The left CST was transected rostral to the decussation using a fine tungsten needle with the basilar artery serving as a landmark for the midline. During the same operation, rats were injected in the cortex/hippocampus contralateral to the lesion with hybridoma cells secreting either mAb IN-1 or anti-HRP as a control antibody. Cyclosporin A (1 mg/100 g body weight, i.p.; Sandimmun; Novartis, Basel, Switzerland) was given daily by intraperitoneal injection during the first 7 days postoperatively to allow the transplants to grow. The control group 2—without transplant—received cyclosporin as well. The sensorimotor cortex of the lesioned CST was injected on the day of operation with the anterograde tracer biotin dextran amine (BDA) by pressure injection (10% BDA in 0.1 M phosphate buffer, pH 7.2; Molecular Probes, Eugene, OR; 2.5 μl into three or four injection sites, mainly in the forelimb area) using a 5-μl Hamilton syringe (Hamilton, Reno, NV). Figure 1A shows a scheme of the experimental design. After surgery and the following day, animals were injected with caprofen (5 mg/kg body weight, subcutaneously; Rimadyl; Pfizer AG, Zurich, Switzerland) as a painkiller and Ringer's solution (i.p.). All experiments were approved by the institution's animal care and use committee (Kantonales Veterinäramt Zürich) and conformed to National Institutes of Health guidelines.

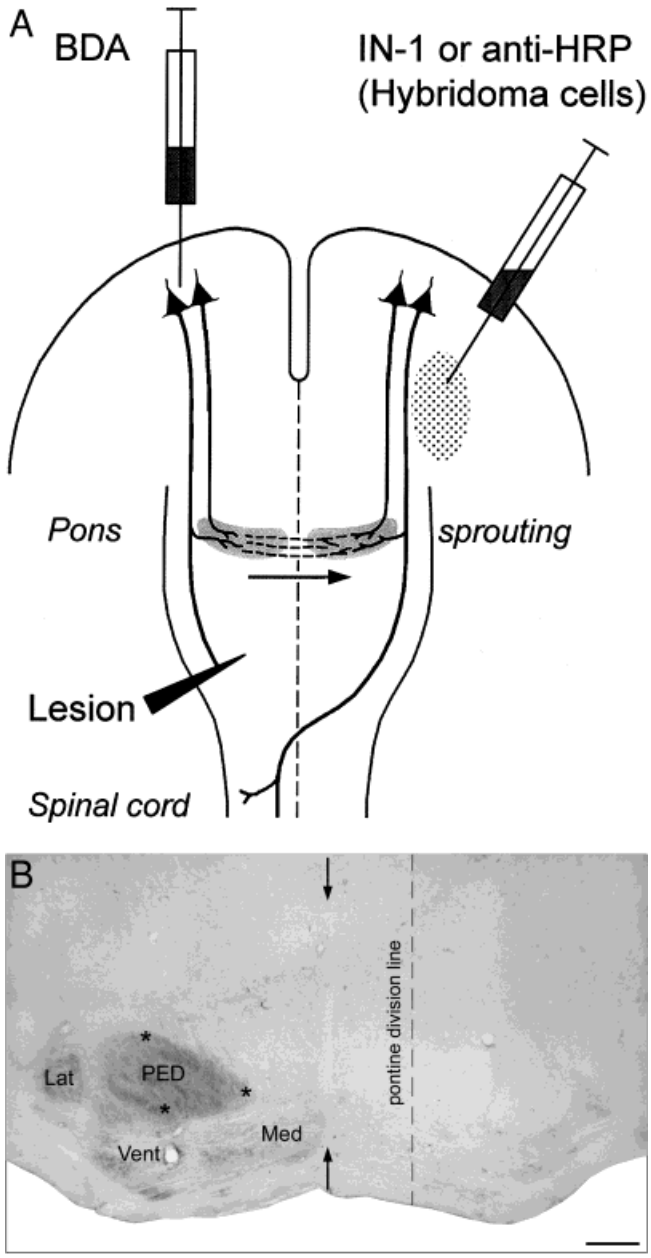

Fig. 1. **A:** Schematic illustration of the experimental design. The corticospinal tracts, the unilateral lesion site, and the injection sites for the tracer biotinylated dextran amine (BDA) and the hybridoma cells are depicted. BDA was injected into the motor cortex ipsilateral to the lesion site to label lesioned corticospinal tract (CST) fibers. The hybridoma cells were injected into the hippocampal region close to the lateral ventricle, contralateral to the tracer and the lesion site, where they form a graft of antibody-producing cells. The dashed lines represent newly sprouted fibers in the pons after the CST lesion and inhibitor-neutralizing antibody 1 (IN-1) application. The arrow indicates the growth direction of the new fibers. Anti-HRP, anti-horseradish peroxidase. **B:** Transverse section containing the basilar pontine nuclei (lateral, Lat; ventral, Vent; medial, Med) and the cerebral peduncle (PED). The midline is indicated by arrows. The pontine division line is taken parallel to the midline and separates the lateral and ventral pontine nucleus from the medial pontine nucleus. This line crosses the medialmost part of the cerebral peduncle that serves as an anatomical landmark. Asterisks in the cerebral peduncle represent the location of the squares where labeled, corticofugal fibers were counted. Scale bar = 360 μm.

Histochemistry

Fourteen days after the BDA injections, all animals were deeply anesthetized with pentobarbital (450 mg/kg, i.p.; Nembutal, Abbott Laboratories, Cham, Switzerland) and perfused transcardially with 100 ml of 0.5 M phosphate buffer (PB), pH 7.4, containing 0.9% NaCl [phosphate-buffered saline (PBS), pH 7.4] and 50,000 UE heparin (Liquemin; Roche, Reinach, Switzerland) followed by 1,000 ml of the fixative (4% paraformaldehyde, 0.1% glutaraldehyde, and 0.2% picric acid in 0.125 M PB, pH 7.4). The brains and spinal cords were removed and postfixed overnight in the same fixative at 4°C. The following day, the pons was removed and embedded in a gelatin-chicken albumin solution polymerized with 25% glutaraldehyde. The tissue was cut on a Vibratome into 50-μm-thick cross sections that were collected in 0.1 M PB and serially mounted on Superfrost-slides (Menzel-Gläser, Germany) according to the semifree-floating technique of Herzog and Brösamle (1997). The sections were washed and incubated overnight at 4°C with an avidin-biotin-peroxidase complex (ABC; Elite kit; 1:100 in 0.1 M PB; Vector Laboratories, Burlingame, CA). The next day, the sections were washed three times for 10 minutes each in 0.1 M PB followed by a 5-minute wash in 0.05 M Tris buffer, pH 8.0. The sections were reacted in 0.05% 3,3′-diaminobenzidine (DAB; Sigma, Buchs, Switzerland) and 0.003% H_2O_2 in 0.05 M Tris buffer, pH 8.0, for about 16 minutes. The process was stopped by washing in 0.1 M PBS, pH 7.4. After three washes in 0.1 M PBS, the sections that were used for light microscopic evaluation were air dried, dehydrated, and coverslipped with Eukitt (Kindler, Freiburg, Germany).

Tissue processing for the electron microscope

After the DAB reaction, sections were postfixed for 1 hour in 2.5% glutaraldehyde in 0.1 M cacodylate buffer, pH 7.4, and subsequently washed in 0.1 M cacodylate buffer. Regions with sprouted fibers were cut out with a razor blade, postfixed for 20 minutes in 2% OsO_4 in cacodylate buffer, and dehydrated in an ascending series of ethanol. A contrast enhancement with 1% uranyl acetate in 70% ethanol was integrated during the dehydration. The tissue was flat embedded in Epon-Araldite (Serva, Heidelberg, Germany). After polymerization at 60°C for 72 hours, the blocks were trimmed, and semithin sections were examined for the presence of labeled axons. Ultrathin sections were cut on an LKB Ultratome (Bromma, Sweden), collected on Pioloform-coated nickel grids (Stork Veco B.V., Eerbeek, Netherlands), and contrasted with Reynold's lead-citrate solution. The sections were air dried and examined in a Zeiss EM 902, electron microscope (EM). Pictures were taken on Scientia EM films (Agfa-Gevaert N.V., Brussels, Belgium) and with a Gatan 792 MultiScan Camera (Pleasanton, CA).

Neuroanatomical analysis

For the light microscopic neuroanatomical analysis, three transverse sections of the basilar pons from each animal were chosen. The most rostral section was taken at the level where the lateral pontine nucleus appears. At an intermediate pontine level, a section was chosen that contained the ventromedial cluster of pontine neurons. The level of the third, more caudally located section was defined by the absence of the ventromedial cluster of pontine neurons and by the appearance of decussating fibers of the trapezoid body. The basilar pons and the cerebral peduncle were outlined, and the midline was indicated using a camera lucida attached to an Olympus microscope (Tokyo, Japan). A vertical line parallel to the midline that divided the basilar pons into a medial part and a lateral part was drawn to anatomically separate the ventral pontine nucleus from the medial pontine nucleus. This pontine division line always crossed the medialmost part of the cerebral peduncle that served as an anatomical landmark and was always located medial to the dense pontine innervation area seen in unilaterally pyramidotomized and IN-1 antibody-treated animals contralateral to the lesion site. The distance between the midline and the pontine division line was about one-third of the distance between the midline and the lateral border of the cerebral peduncle (Fig. 1B). This division is similar to that proposed by Mihailoff et al. (1981). The medial part contained the medial pontine nucleus, and the lateral part contained most of the ventral and lateral pontine nuclei (Fig. 1B).

The cross-sectioned area of the cerebral peduncle was measured using the Neurolucida program (version 2.1; MicroBrightField, Inc., Colchester, VT). Square areas of 29.4 μm × 29.4 μm each were selected at three different locations within the cerebral peduncle (Fig. 1B, asterisks), all labeled corticofugal fibers in these three areas were counted at ×400 magnification, and the total number of labeled fibers per peduncle was calculated. To evaluate the innervation pattern of the basilar pons contralateral to the tracer injection, we evaluated three main features. First, all labeled fibers crossing the midline were counted in all three selected sections and divided by the total number of labeled fibers of the cerebral peduncle for each animal: This value was called the *crossing fiber index*. Second, we counted all of the fibers that crossed the medial-ventral pontine dividing line ventral to the cerebral peduncle. Third, the area with the highest density of labeled fibers in the lateral part of the contralateral basilar pons was selected, a square of 23.5 μm × 23.5 μm was placed in the center of this area, and all labeled axonal structures crossing the borders of this square were counted at a ×1,000 magnification. All results of these three evaluations were normalized for interanimal tracing variability to the number of labeled cerebral peduncle axons, as described above. To examine possible changes in the ipsilateral innervation, the most lateral, ipsilateral innervation field in the ventral pontine nucleus was chosen, and, again, all labeled axonal structures crossing the borders of a square (23.5 μm × 23.5 μm) were counted at ×1,000 magnification. In addition, all bouton-like swellings of the fibers that were located within the square and had a diameter greater than twice the fiber diameter were counted to estimate the number of boutons formed per fiber. The number of boutons on those fibers was divided by the total number of fibers crossing the borders of the square, resulting in a boutons per fiber index (*boutons/fiber index*).

Statistical evaluation

To test the data for significant differences, the two-sample *t*-test assuming unequal variances was used. All data are presented as mean values ± the standard error of the mean (S.E.M.).

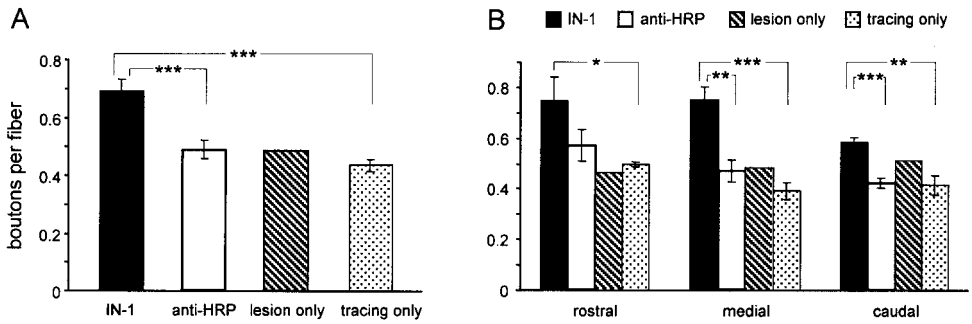

Fig. 2. Quantification of the innervation density in the most lateral corticopontine termination field in the ventral nucleus ipsilateral to the tracer injection and lesion. **A:** Animals that underwent a unilateral pyramidal lesion and received the monoclonal antibody (mAb) IN-1 showed a 40% higher boutons per fiber index than the control groups. **B:** Rostrocaudal distribution of the boutons per fiber index. The significant increase in bouton-like structures in animals in the lesion and mAb IN-1 treatment group was found at all pontine levels. Asterisks indicate significance: single asterisk, $P < 0.05$; double asterisks, $P < 0.01$; triple asterisks, $P < 0.001$.

Figure preparation

Images were assembled in Photoshop software (version 5.5; Adobe Systems, Mountain View, CA). Contrast and brightness levels were adjusted when necessary.

RESULTS

Light microscopic studies

In all groups of animals, the tracer injection was centered in the forelimb area of the motor cortex. To account for interanimal differences in tracing, the number of BDA-positive neurites in the rostral cerebral peduncle was determined for each rat, as described in Materials and Methods. The average number of labeled fibers was not significantly different between the various experimental groups: 9,285 ± 589 axons in the anatomical control group (n = 3 rats; tracing only), 12,180 axons in the group of lesioned animals (n = 2 rats), 13,620 ± 1,342 axons in the lesioned group that was treated with anti-HRP antibody (n = 3 rats), and 11,147 ± 1,176 axons in the group of lesioned animals with IN-1 antibody treatment (n = 6 rats).

Corticopontine innervation: Lesioned side

General innervation pattern. All experimental groups showed an ipsilateral pontine innervation pattern, as in several previous studies (Mihailoff et al., 1978; Wiesendanger and Wiesendanger, 1982; Panto et al., 1995; Z'Graggen et al., 1998). In animals with sharp and exclusive forelimb motor cortex labeling, a single central innervation field was observed at rostral pontine levels within the ventral nucleus; more caudally, an additional small innervation area in the medial part of the pons was found. At caudal pontine levels, the innervation areas were enlarged further, spreading over lateral, ventral, and medial aspects of the basilar pons. These anatomical findings were not influenced by the lesion location or the type of antibody treatment.

Fiber and bouton density. Slight and variable changes in the density of corticopontine fibers in the ventral nucleus of the pons on the side of the CST lesion could be observed after a unilateral CST lesion and antibody treatment; however, this did not reach significance (tracing only group: 0.38; n = 3 rats; lesion only group: 0.72; n = 2 rats; lesion and anti-HRP antibody group: 0.58; n = 3 rats; lesion and IN-1 antibody group: 0.68; n = 6 rats).

The number of bouton-like structures along labeled fibers innervating the ventral pontine nuclei was determined and expressed as the boutons/fiber index (see Materials and Methods). Whereas the lesioned animals showed at best a trend for an increase, animals with CST lesion and IN-1 antibody treatment showed a robust increase of about 40% in the boutons/fiber index at all levels of the pons (Fig. 2). Control antibody-treated rats never showed such an effect.

Corticopontine fibers crossing the midline: Innervation of the contralateral pons

General innervation pattern. In normal adult rats, only a very minor group of corticopontine fibers projects to the contralateral basilar pontine nuclei, mainly at midpontine and caudal levels (Wiesendanger and Wiesendanger, 1982; Panto et al., 1995; Z'Graggen et al., 1998). Unilateral pyramidotomy combined with IN-1 antibody treatment resulted in changes of the contralateral basilar pontine nuclei innervation: An increased number of fibers crossing the midline and a dense contralateral innervation of the ventral pontine nucleus were found (Fig. 3D–F). This contralateral projection was distributed to the mirror image location of the typical corticopontine projection zones. The density of this new contralateral innervation, however, was always less than the ipsilateral innervation of the corresponding area. In the animals that received unilateral pyramidotomy alone or with anti-HRP antibody treatment, sprouting of some fibers that projected to the contralateral medial pontine nucleus and innervation of a zone near the midline at a very low density were observed (Fig. 3A–C). To investigate this compensatory sprouting after a unilateral pyramidotomy in more detail, we quantified the number of midline-crossing corticopontine fibers, their spread to the ventral pontine nucleus, and the density of the terminal plexus formed.

Midline-crossing corticopontine fibers. Corticopontine fibers from the lesioned side of the brain crossed the midline either at the level of the ventral part of the pons (white matter, where axons of pontine neurons cross to the contralateral side before they ascend as mossy fibers to

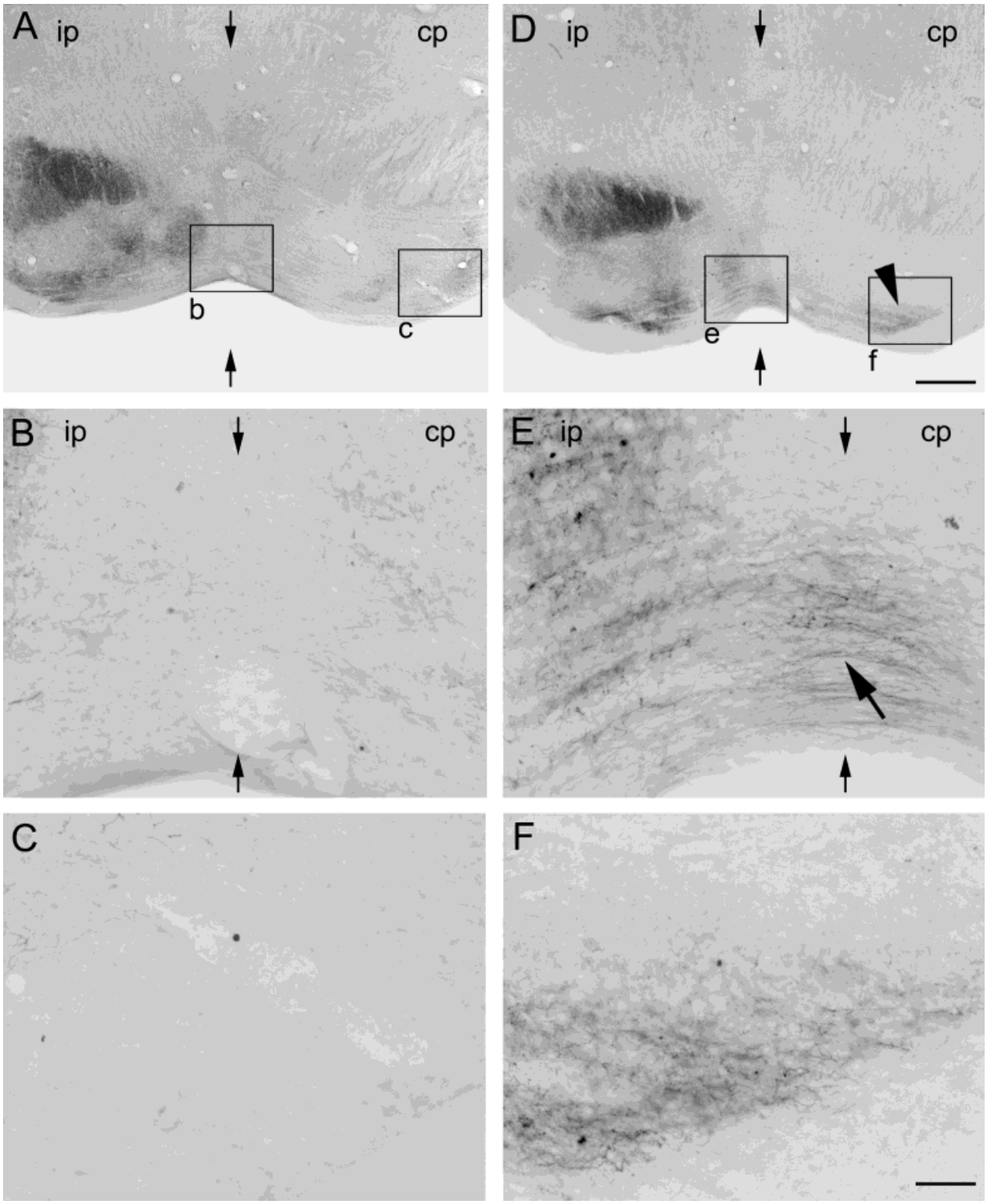

Fig. 3. Cross sections through the basilar pontine nuclei. Photomicrographs on the left (**A–C**) show BDA-labeled corticofugal fibers from lesioned animals that received a control antibody (anti-HRP), and photomicrographs on the right (**D–F**) show sections with traced fibers from lesioned, mAb IN-1-treated animals. Enlargements of the areas boxed (b, c, e, and f) are shown in B, E (midline), C, and F (ventral pontine nucleus of the contralateral pons). A–C: In lesioned, anti-HRP-treated animals, only very few fibers innervate the contralateral pons (cp; right lower half of A). Crossing fibers are rare in the midline (B) and in the ventral pontine nuclei of the contralateral pons (C). D–F: Lesioned animals that received mAb IN-1 showed an increased projection from the ipsilateral pons (ip) to the contralateral pons (cp; arrowhead). At higher magnification, the midline-crossing fibers (E, large arrow) and the contralateral innervation field in the ventral pontine nucleus (F) 2 weeks after IN-1 treatment and unilateral pyramidotomy are seen. Arrows indicate the midline. Scale bars = 360 μm in D (also applies to A); 60 μm in F (also applies to B,C,E,).

the cerebellum) or directly between the basilar pontine nuclei (gray matter). Normal animals, rats with CST lesion alone, or lesioned, control antibody-treated rats had only very few corticopontine fibers crossing the midline (Figs. 3C, 5A,B). In the pons of lesioned animals that were treated with IN-1, however, about three times more corticopontine fibers crossing the midline were found (Figs. 3E, 4C, 5A). Similar to what was seen in normal rats, the number of crossing fibers increased from rostral to caudal pontine levels (Fig. 5B). The few crossing fibers in the lesioned, anti-HRP antibody-treated and the lesion-only group ended in an area close to the midline. All labeled fibers in this area were very thin, forming a diffuse innervation field of very low density. In lesioned, IN-1-treated animals, this innervation area also was present, but many labeled fibers projected straight and laterally through this area to arborize and terminate in more lateral regions (ventral pontine nucleus; Fig. 3F).

Crossed fiber projection to the lateral part of the pons. To examine which parts of the contralateral pons were reached by the midline-crossing fibers, a vertical line was drawn separating the medial part from the more lateral parts of the nuclear complex (Fig. 1B). All labeled fibers crossing this pontine division line were counted at the three pontine levels. Fibers crossing this line reached at least the ventral pontine nucleus and also may project to more lateral regions. In normal animals, only very few fibers were seen to cross the medial-lateral division line, even at most caudal pontine levels. Pyramidotomy, especially when combined with a control antibody-secreting hybridoma transplant, showed a small increase in the number of laterally growing fibers (Fig. 5C). The lesioned, IN-1 antibody-treated animals had about twice as many fibers crossing the medial-lateral division line; this increase was significant at all pontine levels and increased from rostral levels to caudal levels (Fig. 5C,D).

Innervation density of contralateral pontine nuclei. In each examined cross section, the area in the lateral part of the pons that contained the densest innervation by crossing corticopontine fibers was evaluated quantitatively for fiber density (see Materials and Methods, above). There were no significant differences between normal animals, pyramidotomy alone animals, and lesioned, control (anti-HRP) antibody-treated rats at rostral levels (Fig. 5F). At midpontine and caudal levels, the lesioned control groups had slightly higher fiber densities (Fig. 5F). The innervation index of the lesioned, IN-1 antibody-treated group, in which the highest labeling density was always located in the lateral part of the ventral pontine nucleus, was at least two times higher than in the other groups (Fig. 5E). An example of the innervation density in a lesioned, IN-1 antibody-treated animal is shown in Figure 4A (ipsilateral to the lesion) and Figure 4B (contralateral to the lesion). This increase of innervation density showed a rostral-to-caudal gradient, similar to the number of midline-crossing fibers (Fig. 5F).

Ultrastructural studies

General findings. At the ultrastructural level, BDA labeling was characterized by the presence of an electron-dense DAB reaction product filling the entire cytoplasm of the labeled axons or terminals (Fig. 6). Cell organelles, such as mitochondria, endoplasmic reticulum, and synaptic vesicles, remained free of label. Ultrathin sections of the pons showed the known distribution of fibers and neuronal somata (Mihailoff et al., 1981). At the ventral border, bundles of strongly myelinated fibers, the fibrae transversae, formed the efferent system of the pons that projects as mossy fibers to the contralateral cerebellar hemisphere. Between the cerebral peduncle and this ventral white matter, clusters of pontine neurons alternated with bundles of fibers, most of them myelinated. Within the clusters of these pontine neurons, unmyelinated axonal and dendritic profiles were present. Synaptic profiles that were found in the pons were asymmetric and contained round vesicles of various sizes.

Labeled axonal and presynaptic structures. The lateral part of the ventral pontine nuclei contralateral to the pyramidal lesion and the tracer injection was analyzed for labeled axons and synapses in mAb IN-1-treated animals. Most of these labeled, crossed corticopontine axons were of small diameter (from 0.04 μm up to 0.29 μm; most were between 0.15 μm and 0.25 μm if no mitochondrial profiles were present, whereas neurites containing mitochondria had diameters up to 0.53 μm). It is noteworthy that none of the labeled axons was myelinated (consistently in five animals; approximately ten labeled fibers per section), in contrast to many labeled myelinated axons in pontine innervation fields ipsilateral to the tracer injection (data not shown). Vesicle-like structures that were seen in the labeled axons often were round and had the same size as the vesicles seen in labeled synapses.

Labeled synapses, frequently in the vicinity of labeled axonal profiles, showed a high variability in size and often very irregular shapes (Fig. 6). Most of them were large, and they contained up to six mitochondrial profiles. Compared with neighboring, unlabeled presynaptic structures, the number of mitochondria in these labeled, presumably newly formed synapses appeared to be increased. The synaptic vesicles were homogeneous in size (25–40μm) and round in shape. All examined labeled boutons formed asymmetric synaptic contacts on dendritic processes, often on dendritic spines (Fig. 6). Axosomatic contacts on basilar pontine neurons were not found. Labeled synapses were found almost exclusively in lesioned, mAb IN-1-treated animals; about ten labeled fibers and three or four synapses were found per EM section (0.5 mm × 0.5 mm) of the lateral pons of mAb IN-1-treated animals (n = 5 rats).

DISCUSSION

In this report, we provide evidence for lesion-induced sprouting of corticopontine fibers after mAb IN-1 treatment in adult rats. The fibers sprouted across the pontine midline and established new synapses contralateral to the lesion and tracer injection site. The novel synapses showed the same ultrastructural characteristics that are seen in normal corticopontine synaptic endings.

A unilateral pyramidotomy in adult mammals leads to long-lasting functional impairments of fine motor control of the forelimbs, as shown in previous studies. No functional recovery of precision movements and little or no anatomical plasticity were found after such lesions in mature animals (Kuang and Kalil, 1990). Masking of the myelin-associated neurite growth inhibitor Nogo-A by mAb IN-1 resulted in major structural rearrangements and an almost complete functional recovery in several behavioral tasks (Thallmair et al., 1998; Z'Graggen et al., 1998).

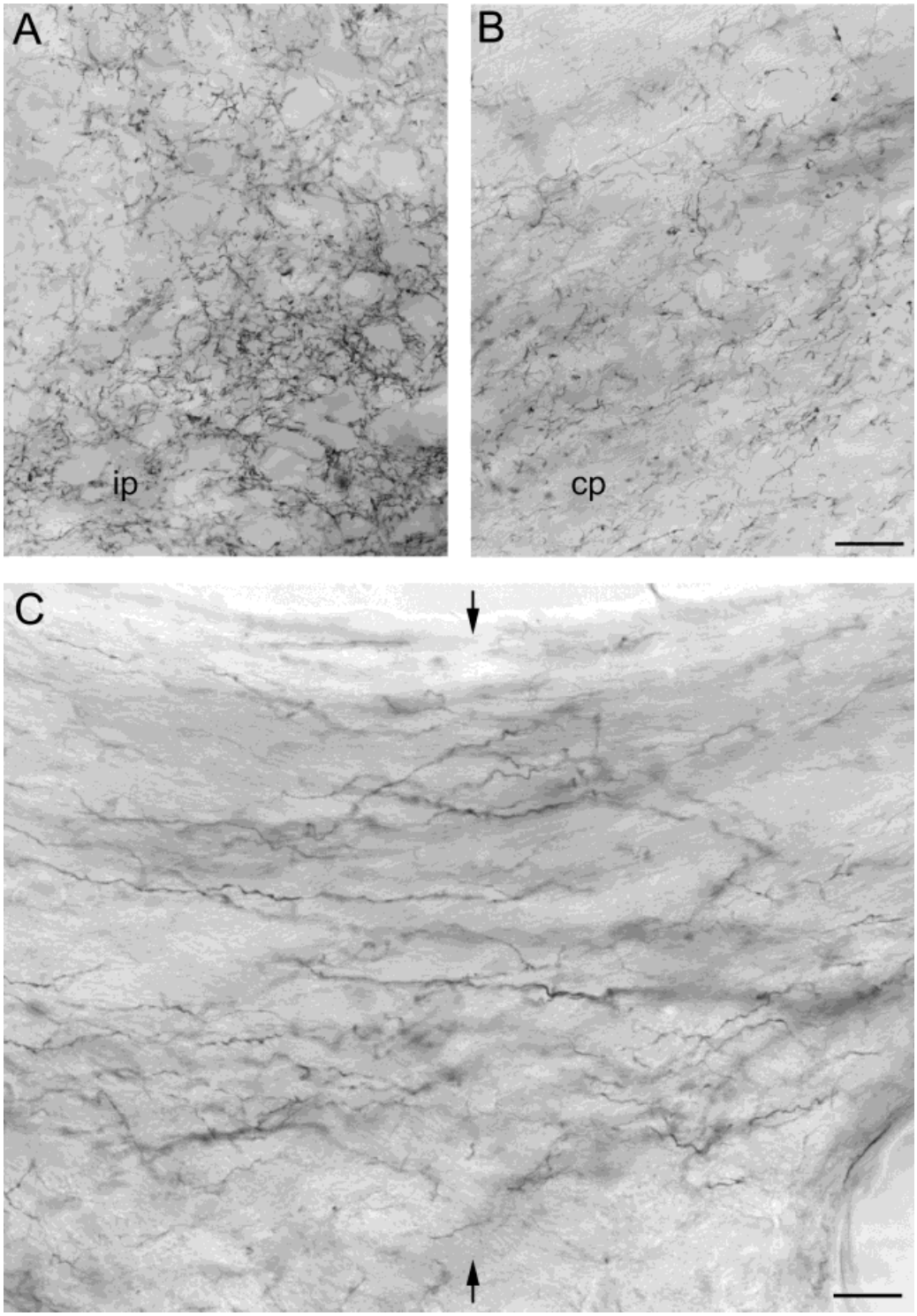

Fig. 4. **A,B:** High magnification views of cross sectional areas of the ipsilateral pontine (ip; A) and the contralateral pontine (cp; B) innervation zone in the ventral pontine nucleus in an IN-1 antibody-treated, lesioned animal. **C:** Midline-crossing fibers. Arrows indicate the midline. Scale bars = 60 μm in B (also applies to A); 20 μm in C.

The treatment with the IN-1 antibody resulted in an increase of the midline-crossing fibers, of fibers growing to more lateral regions of the contralateral pons, and of the contralateral pontine innervation density. This new contralateral innervation resembled the innervation of the ipsilateral basilar pons, which is organized somatotopi-

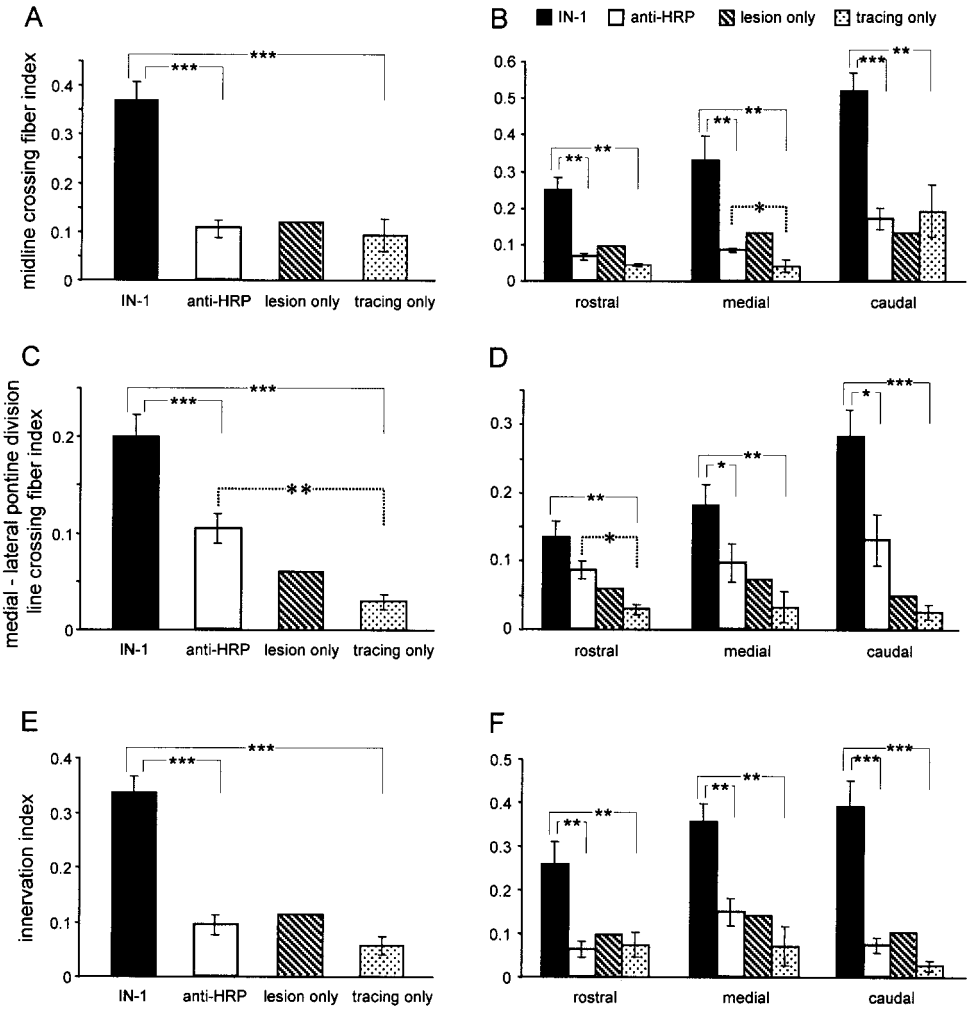

Fig. 5. Three main features were evaluated to quantify the innervation of the basilar pons contralateral to the lesion and the tracer injection site. **A:** Quantification of pontine midline-crossing fibers. In mAb IN-1-treated animals, a three-fold increase of midline-crossing fibers was found, whereas the anti-HRP-treated and lesion-only animals showed values similar to those found in normal rats (tracing only). **B:** Like the normal animals, the number of midline-crossing fibers increased from rostral to caudal pontine levels. At every pontine level, the IN-1 group showed significantly more midline-crossing fibers than the control groups. **C:** To determine which parts of the contralateral pons were reached by the midline-crossing fibers, all axons crossing the pontine division line were counted. The unilateral pyramidal lesion, especially when combined with an anti-HRP antibody treatment, resulted in a small increase in the number of laterally growing fibers. The lesioned, IN-1 antibody-treated animals, however, showed almost twice as many fibers crossing this lateral line. **D:** The number of fibers crossing the pontine division line increased from rostral to caudal, similar to the number of midline-crossing fibers. This increase was significant for the mAb IN-1-treated and anti-HRP-treated animals at all pontine levels. **E:** Pyramidotomy in combination with IN-1 antibody treatment led to an at least two-fold increase in the innervation index, whereas there were no significant differences between the control groups. **F:** The innervation index was significantly enhanced in mAb IN-1-treated animals at all pontine levels, with a slight trend toward higher values from rostral to caudal. Asterisks indicate significance: single asterisk, $P < 0.05$; double asterisks, $P < 0.01$; triple asterisks, $P < 0.001$ (t test).

cally (Mihailoff et al., 1978; Wiesendanger and Wiesendanger, 1982; Panto et al., 1995). Animals that showed such structural plasticity in the pons and sprouting in the cervical spinal cord recovered almost completely in a food-pellet reaching paradigm, a behavioral task that required fine motor control (Z'Graggen et al., 1998).

The new BDA-labeled axons and terminals contralateral to the lesion and tracer injection site most likely represent sprouted corticofugal fibers; such fibers were virtually absent in normal and lesioned control animals. However, we cannot exclude the possibility that some of the labeled fibers and boutons in the contralateral basilar pontine nuclei may represent the normal crossed corticopontine projection, which is very small (Wiesendanger and Wiesendanger, 1982; Panto et al., 1995; Z'Graggen et al., 1998). In addition, we showed fibers and boutons in regions of the pons that typically do not receive the normal crossed projection. Thus, we suggest that normal crossed projections play a minor role in the expansion of the contralateral terminal fields after lesion and IN-1 antibody treatment. The increase of midline-crossing fibers in the pons may be derived from fibers that are redirected to the contralateral pons or from neurites that formed new collaterals to innervate the contralateral pontine nuclei.

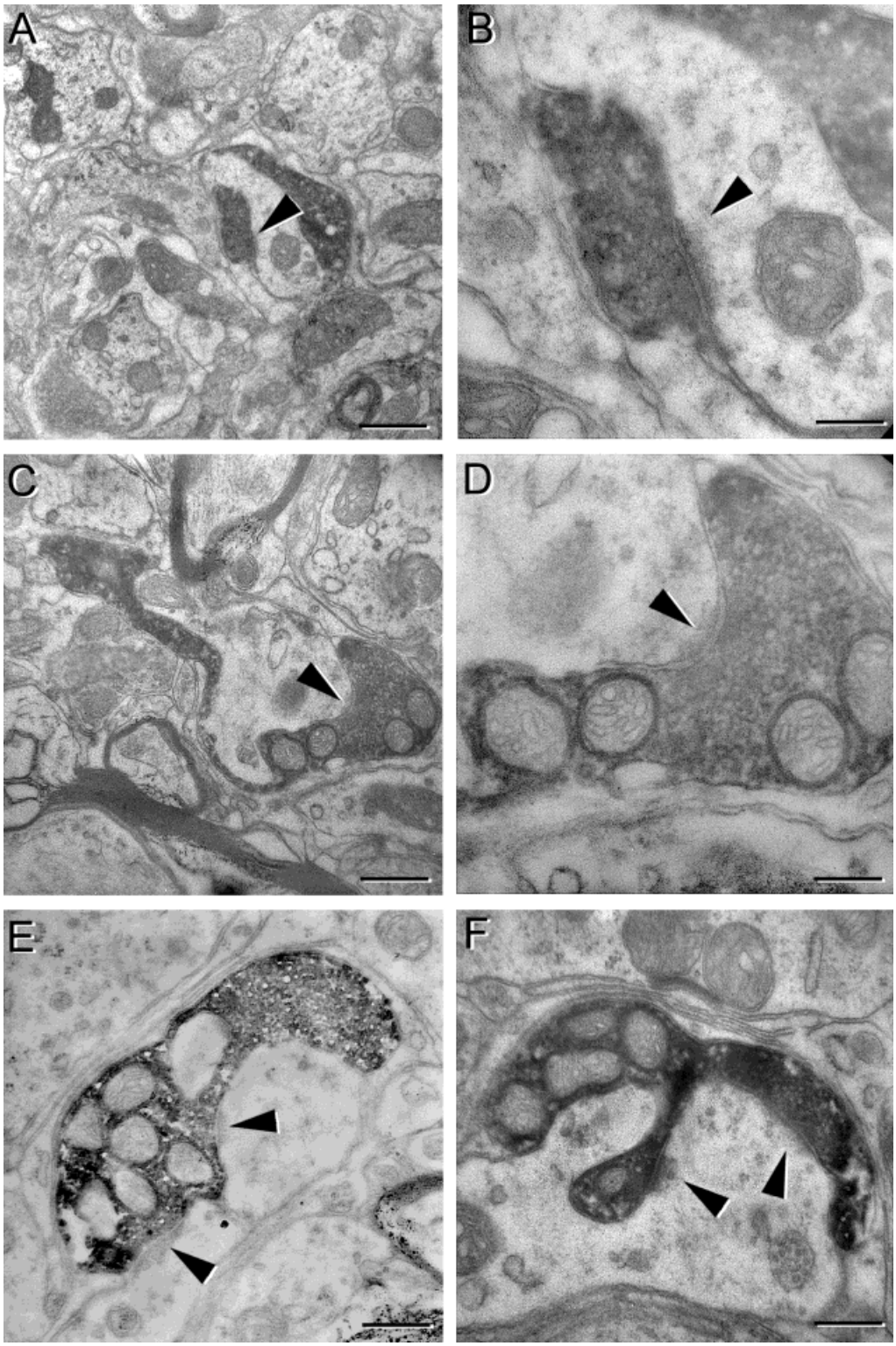

Fig. 6. Representative examples of boutons filled with 3,3′-diaminobenzidine (DAB) reaction product located in the ventral pontine nucleus contralateral to the lesion and the tracer injection site in IN-1 antibody-treated animals. All boutons contained round vesicles. They formed asymmetric synaptic sites (arrowheads) and contacted dendritic processes. **A:** Overview of a region in the ventral pontine nucleus with a labeled synapse. **B:** Higher magnification of the synapse depicted in A. **C:** Unmyelinated axon filled with DAB reaction product with terminal synaptic site. **D:** Higher magnification of the synapse depicted in C. The synaptic cleft, the electron-dense active zone, and the round vesicles are illustrated. **E,F:** Note the irregular shapes of these synapses, both of which show two active sites and contain several mitochondrial profiles. Scale bars = 2.5 μm in A; 0.7 μm in B; 1.6μm in C; 0.6 μm in D; 1.1 μm in E; 0.4 μm in F.

The new midline-crossing fibers terminated topographically in the contralateral basilar pontine nuclei, and the EM results showed that the synapses formed by these midline-crossing fibers had the typical structural characteristics of corticopontine boutons (Mihailoff and McArdle, 1981). The synaptic contacts were asymmetric (Gray's type I; Gray, 1959) and the boutons contained round vesicles (rat: Mihailoff and McArdle, 1981; cat: Holländer et al., 1969). Considering these structural characteristics, we suggest that the new synapses belong to Mihailoff and McArdle's (1981) category 1 of pontine terminal endings. The finding of new synapses with the typical characteristics of corticopontine presynaptic profiles in the contralateral pons after a unilateral lesion corroborates earlier EM reports in which axonal sprouting in the corticopontine system was described after neonatal cortical lesions (Leong, 1976; Mihailoff and Castro, 1981). The new synapses terminated exclusively on dendrites, as described previously for normal synaptic contacts of the same category (Brodal, 1968; Holländer et al., 1969; Mihailoff and McArdle, 1981).

Neutralization of the myelin-associated neurite growth inhibitor Nogo-A also resulted in some lesion-induced changes in the ipsilateral pons. In the ipsilateral medial pontine nuclei, the fiber density showed a small and variable increase after lesion alone and in combination with antibody treatment. A similar weak increase in fiber density has been found in the ipsilateral pons after a unilateral pyramidotomy in the neonatal and adult rat in a previous report (Z'Graggen et al., 2000). In our study, however, we found a significantly enhanced bouton/fiber index in the ipsilateral pons in mAb IN-1-treated animals after a unilateral pyramidal lesion, reflecting sprouting and possibly reinforcement of ipsilateral corticopontine connections.

The lesion-induced changes of the corticopontine innervation described here probably are due to and influenced by a variety of factors in addition to the neutralization of the neurite growth inhibitor Nogo-A. Functional imbalance of the motor and sensory systems caused by the lesion may lead to an up-regulation of growth-promoting, guidance, and survival factors (Wizenmann et al., 1993; Thoenen, 1995). The nature of these factors in the corticopontine system is not known at the moment. The information for the formation of new, characteristic corticopontine synapses also must be present or reexpressed in these adult animals.

The anatomical results presented here were obtained 2 weeks after the lesion and implantation of the antibody-secreting hybridoma cells. Thus, the structural changes occurred rapidly, and, most likely, these rearrangements remain stable over time, as shown in a previous study from our laboratory (Z'Graggen et al., 1998). The precise time course of sprouting, synapse formation, and possibly also retraction phenomena is not known. Corticopontine fibers may be rerouted or may give rise to new collaterals. When new synapses are formed, a phase of activity-driven refinement may follow and, finally, the elimination of exuberant or wrong connections. Some of the fibers terminating in the pons are collaterals of corticospinal fibers (Ugolini and Kuypers, 1986; Akintunde and Buxton, 1992). The transection of these fibers by the pyramidal lesion may lead to a compensatory sprouting across the pontine midline (Sabel and Schneider, 1988; "pruning effect"). In addition, the unilateral pyramidal lesion denervates half of the spinal cord and the dorsal column nuclei ipsilateral to the lesion, which may cause a functional imbalance of the motor and sensory systems. Activity-driven up-regulation of neurotrophic or growth-promoting factors may induce the formation of new collaterals, enhanced terminal arborizations, and new synapses in the pontine nuclei.

Recently, a new additional role of Nogo-A has been found (Zagrebelsky et al., 1998): Myelin-associated neurite growth inhibitors seem to actively suppress the expression of growth-associated genes in adult central neurons. Thus, the application of neutralizing antibodies not only may provide a growth-permissive microenvironment by locally masking the myelin-associated neurite growth inhibitor Nogo-A but also may lead to an up-regulation of growth-associated gene expression in the cell body.

In a previous study, we showed that a very high degree of functional recovery takes place after unilateral pyramidotomy and treatment with mAb IN-1 (Z'Graggen et al., 1998). The sprouted fibers and the new synapses described here in the pons, as well as other plastic rearrangements in the brainstem, brain, and spinal cord (Thallmair et al., 1998), probably contribute and collaborate to restore fine movements in these unilaterally lesioned, anti-Nogo-A antibody-treated adult animals.

LITERATURE CITED

Akintunde A, Buxton DF. 1992. Origins and collateralization of corticospinal, corticopontine, corticorubral and corticostriatal tracts: a multiple retrograde fluorescent tracing study. Brain Res 586:208–218.

Barth TM, Stanfield BB. 1990. The recovery of forelimb-placing behavior in rats with neonatal unilateral cortical damage involves the remaining hemisphere. J Neurosci 10:3449–3459.

Bregman BS, Kunkel-Bagden E, Schnell L, Dai HN, Gao D, Schwab ME. 1995. Recovery from spinal cord injury mediated by antibodies to neurite growth inhibitors. Nature 378:498–501.

Brodal P. 1968. The corticopontine projection in the cat. I. Demonstration of a somatotopically organized projection from the primary sensorimotor cortex. Exp Brain Res 5:210–234.

Caroni P, Schwab ME. 1988a. Antibody against myelin-associated inhibitor of neurite growth neutralizes nonpermissive substrate properties of CNS white matter. Neuron 1:85–96.

Caroni P, Schwab ME. 1988b. Two membrane protein fractions from rat central myelin with inhibitory properties for neurite growth and fibroblast spreading. J Cell Biol 106:1281–1288.

Chen MS, Huber AB, van der Haar ME, Frank M, Schnell L, Spillmann AA, Christ F, Schwab ME. 2000. Nogo-A is a myelin-associated neurite outgrowth inhibitor and an antigen for monoclonal antibody IN-1. Nature 403:434–439.

Gray EG. 1959. Axo-somatic and axo-dendritic synapses of the cerebral cortex: electron microscope study. J Anat 93:420–433.

Herzog A, Brösamle C. 1997. Semifree-floating treatment—a simple and fast method to process consecutive sections for immunohistochemistry and neuronal tracing. J Neurosci Methods 72:57–63.

Holländer H, Brodal P, Walberg F. 1969. Electron microscopic observations on the structure of the pontine nuclei and the mode of termination of the corticopontine fibers. An experimental study in the cat. Exp Brain Res 7:95–110.

Kalil K, Reh T. 1982. A light and electron microscopic study of regrowing pyramidal tract fibers. J Comp Neurol 211:265–275.

Kapfhammer JP. 1997. Restriction of plastic fiber growth after lesions by central nervous system myelin-associated neurite growth inhibitors. Adv Neurol 73:7–27.

Kartje-Tillotson G, Neafsey EJ, Castro AJ. 1986. Topography of corticopontine remodelling after cortical lesions in newborn rats. J Comp Neurol 250:206–214.

Kennard MA. 1936. Age and other factors in motor recovery from precentral lesions in monkeys. Am J Physiol 115:138146.

Kennard MA. 1938. Reorganization of motor function in the cerebral cortex

of monkeys deprived of motor and premotor areas in infancy. J Neurophysiol 1:477–496.

Kuang RZ, Kalil K. 1990. Specificity of corticospinal axon arbors sprouting into denervated contralateral spinal cord. J Comp Neurol 302:461–472.

Leong SK. 1976. A qualitative electron microscopic investigation of the anomalous corticofugal projections following neonatal lesions in the albino rats. Brain Res 107:1–8.

Mihailoff GA, Castro AJ. 1981. Autoradiographic and electron microscopic degeneration evidence for axonal sprouting in the rat corticopontine system. Neurosci Lett 21:267–273.

Mihailoff GA, McArdle CB. 1981. The cytoarchitecture, cytology, and synaptic organization of the basilar pontine nuclei in the rat. II. Electron microscopic studies. J Comp Neurol 195:203–219.

Mihailoff GA, Burne RA, Woodward DJ. 1978. Projections of the sensorimotor cortex to the basilar pontine nuclei in the rat: an autoradiographic study. Brain Res 145:347–354.

Mihailoff GA, McArdle CB, Adams CE. 1981. The cytoarchitecture, cytology, and synaptic organization of the basilar pontine nuclei in the rat. I. Nissl and Golgi studies. J Comp Neurol 195:181–201.

Panto MR, Cicirata F, Angaut P, Parenti R, Serapide F. 1995. The projection from the primary motor and somatic sensory cortex to the basilar pontine nuclei. A detailed electrophysiological and anatomical study in the rat. J Hirnforsch 36:7–19.

Raineteau O, Z'Graggen WJ, Thallmair M, Schwab ME. 1999. Sprouting and regeneration after pyramidotomy and blockade of the myelin-associated neurite growth inhibitors NI 35/250 in adult rats. Eur J Neurosci 11:1486–1490.

Sabel BA, Schneider GE. 1988. The principle of "conservation of total axonal arborizations": massive compensatory sprouting in the hamster subcortical visual system after early tectal lesions. Exp. Brain Res 73:505–518.

Schnell L, Schwab ME. 1990. Axonal regeneration in the rat spinal cord produced by an antibody against myelin-associated neurite growth inhibitors. Nature 343:269272.

Schnell L, Schwab ME. 1993. Sprouting and regeneration of lesioned corticospinal tract fibres in the adult rat spinal cord. Eur J Neurosci 5:1156–1171.

Schwab ME, Kapfhammer JP, Bandtlow CE. 1993. Inhibitors of neurite growth. Annu Rev Neurosci 16:565–595.

Thallmair M, Metz GAS, Z'Graggen WJ, Raineteau O, Kartje GL, Schwab ME. 1998. Neurite growth inhibitors restrict plasticity and functional recovery following corticospinal tract lesions. Nat Neurosci 1:124–131.

Thoenen H. 1995. Neurotrophins and neuronal plasticity. Science 270:593–598.

Ugolini G, Kuypers HG. 1986. Collaterals of corticospinal and pyramidal fibres to the pontine grey demonstrated by a new application of the fluorescent fibre labelling technique. Brain Res 365:211–227.

Whishaw IQ, Kolb B. 1988. Sparing of skilled forelimb reaching and corticospinal projections after neonatal motor cortex removal or hemidecortication in the rat: support for the Kennard doctrine. Brain Res 451: 97–114.

Wiesendanger R, Wiesendanger M. 1982. The corticopontine system in the rat. II. The projection pattern. J Comp Neurol 208:227–238.

Wizenmann A, Thies E, Klostermann S, Bonhoeffer F, Bahr M. 1993. Appearance of target-specific guidance information for regenerating axons after CNS lesions. Neuron 11:975–983.

Zagrebelsky M, Buffo A, Skerra A, Schwab ME, Strata P, Rossi F. 1998. Retrograde regulation of growth-associated gene expression in adult rat Purkinje cells by myelin-associated neurite growth inhibitory proteins. J Neurosci 18:7912–7929.

Z'Graggen WJ, Metz GAS, Kartje GL, Thallmair M, Schwab ME. 1998. Functional recovery and enhanced corticofugal plasticity after unilateral pyramidal tract lesion and blockade of myelin-associated neurite growth inhibitors in adult rats. J Neurosci 18:4744–4757.

Z'Graggen WJ, Fouad K, Raineteau, O, Metz GAS, Schwab ME, Kartje GL. 2000. Compensatory sprouting and impulse rerouting after unilateral pyramidal tract lesion in neonatal rats. J Neurosci 20:6561–6569.